scientific reports

Check for updates

OPEN

# Multiband antenna design method using predefined shapes and image segmentation techniques for IoT applications

Fan Jiang[1], Zhen Zhang[2]✉, Bo Liu[3] & Weihua Yu[4]✉

**The development of the internet of things necessitates more compact electronic products. This paper proposes a novel approach: designing a predefined shape to function as a antenna without changing its visual appearance. By comparing with the defined threshold, an example of university emblem image is transformed into a binarized image, then define the conductive metal and dielectric substrates. The metallic part are pixelated, ports are added between adjacent pixels, and the initial structure's port impedance matrix is derived through full electromagnetic simulation, forming a multi-port network model. The target three bands are: WiFi 2.4 GHz (2.4–2.5 GHz), LTE FDD Band 3400 (3.4–3.5 GHz), and FR1 n79 band (4.7–4.9 GHz). Leveraging the port impedance matrix, we employ a genetic algorithm to optimize the pixel connectivity, meeting the defined design specifications. The resulting patch antenna, retaining the appearance of the university emblem, achieves 12.9%/22.8%/7.0% bandwidths, 3.6/4.6/3.0 dBi gains, and > 75% efficiency, thereby validating the proposed method.**

**Keywords** Internet of things, Image segmentation, Logo antenna, Multi-port network, Patch antenna, Predefined shape

Miniaturization holds significant importance in antenna design. Whether designing individual antenna elements or entire arrays, a common strategy for compact antenna design involves adopting standardized shapes. For instance, circular structures[1], triangular antenna elements[2], and rectangular antenna elements[3] are frequently employed. Additionally, techniques such as integrating triangular grooves[2] and complementary split-ring structures[4] are utilized to enhance performance, particularly the isolation between adjacent antennas. Such designs not only improve the performance of antenna elements but also improve isolation within antenna arrays and other relevant aspects. If the antenna design can be completed using the predefined shape instead of making a customized design specifically for the antenna, it will further improve the efficiency and miniaturization of the antenna design and save the occupied space.

The design of an antenna in the form of a 2D image represents an innovative concept that preserves the appearance of the brand while integrating additional wireless communication functionalities. This dual-function design enhances the product's practicality and efficiency, therefore eliminating the need for additional separate antenna components. Consequently, it achieves a more miniaturized design[5–8] while preserving the overall aesthetics of the product[9,10]. A major challenge in implementing this idea is that real-life objects have predefined shapes that cannot be easily changed, and these shapes have a significant impact on antenna performance. To address this challenge, this work proposes converting the 2D image of the logo into a fixed-size, multi-band patch antenna[11–14] specifically designed to operate across customized, multiple frequency bands, making it ideally suited for mobile devices.

To our knowledge, there are only a limited number of related research works available in this area[5,7,15–17], and the existing design methods are largely ad-hoc, lacking a comprehensive and generalized design approach. For instance, in[6], the predefined shape of the Louis Vuitton logo is utilized for antenna designs, but only for specific structural configurations. An efficient optimization algorithm is proposed in[17]. At present, there is an absence of comprehensive methods that include the extraction of image data, its conversion to antenna structure, and the

[1]School of Physics and Optoelectronic Engineering, Guangdong University of Technology, Guangzhou 510006, China. [2]School of Electronics and Communication Engineering, Guangzhou University, Guangzhou 510006, China. [3]James Watt School of Engineering, University of Glasgow, Glasgow G12 8QQ, UK. [4]School of Integrated Circuits and Electronics, Beijing Institute of Technology, Beijing 100081, China. ✉email: zhangzhen@gzhu.edu.cn; ywhbit@bit.edu.cn

optimization of the antenna design. Moreover, achieving miniaturization and lightweight design is essential for modern portable and wearable devices[18], yet these considerations have not been deeply explored in[6,7,15–17]. In addition, for some complex predetermined shapes, fine electromagnetic simulation mesh settings are needed to ensure high simulation accuracy, but this increases the computational cost of optimization.

To address these challenges, a new method, called the predefined shape multiband patch antenna design method based on image segmentation and multi-port networks, is proposed. The aims include: (1) providing high-quality multiband antenna performances, (2) general to almost all kinds of predefined shapes, (3) fast design speed, i.e., the optimization time is within a few hours.

The main idea of the proposed approach is as follows. For any 2D image representing a real-world object, image segmentation techniques[19,20] are firstly used to extract the desired shape for the patch antenna. Based on the segmented image, a multi-port network model[21–23] is built, which is accurate and has a low computing cost (i.e., less than 1 s for each simulation). Genetic algorithm (GA)[21] is then applied in optimization. The performance is demonstrated by a tri-band patch antenna operating across the band of 2.4–2.5 GHz, 3.3–3.4 GHz, and 4.7–4.9 GHz using the predefined shape of the badge of Guangzhou University, China.

The remainder of this letter is organized as follows: Section II presents a detailed elaboration of the proposed method. Section III introduces the antenna design with the badge of Guangzhou University, which serves as a demonstration of the method, along with the corresponding measurement results. Finally, Section IV provides the conclusions.

## The proposed method

As illustrated in Fig. 1, the proposed method includes three stages: image extraction, antenna configuration and antenna geometry optimization, as described in Section II.A, II.B and II.C respectively.

### Image extraction

The first step is to convert the predefined 2D image to the antenna geometry. The color is expressed by three components: $R(i, j)$, $G(i, j)$, and $B(i, j)$, with values ranging from 0 to 255 for each component. Firstly, grayscale processing is used to reduce the redundant information in the color image. The specific method is to take the maximum value of the brightness component of the three colors of the image as the gray value.

$$Gr\,(i,j) = \max\left\{R\,(i,j)\,, G\,(i,j)\,, B\,(i,j)\right\} \tag{1}$$

$Gr(i, j) = \max\{ R(i, j), G(i, j), B(i, j)\}$. (1)

where $Gr$ ranges from 0 to 255, encompassing a total of 256 possible values. For the obtained gray image, it is further converted into a binary image through image threshold segmentation. In this binary image, the values of 0 and 1 represent the absence and presence of metal patches, respectively, thereby defining the antenna's geometry. This process is defined as

$$p\,(i,j) = \begin{cases} 1 \;if Gr\,(i,j) > \alpha \\ 0 \;otherwise \end{cases} \tag{2}$$

.

where $\alpha$ is the threshold, which is user-defined.

### Antenna configuration

Once the image is extracted, it is necessary to transform the 2D image into the physical structure of the antenna. The antenna structure comprises dielectric substrates, metal ground, and radiation metal patches. Therefore, we select a suitable dielectric substrate to place radiation metal patches and metal grounds. A selected portion of the image is mapped to a metal ground, while the other portion is mapped to a radiating metal patch. As the physical size of the antenna is related to its operating frequency, we determine the size of the antenna based on its expected operating frequency band. The specific steps for converting the pixel matrix of the 2D image into an antenna structure are as follows:

***Step 1*** Estimate the expected operating wavelength λ of the antenna at the minimum operating frequency.

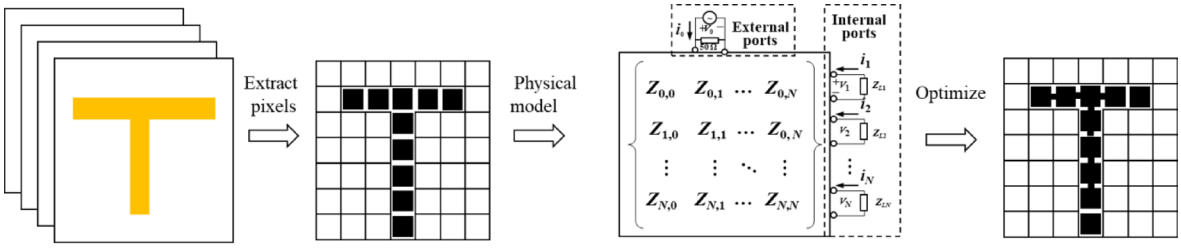


**Fig. 1**. The proposed design framework of the multi-band patch antenna. (**a**) 2-D images (**b**) Initial antenna structure (**c**) Multi-port network model, and (**d**) Optimization of antenna performance.

***Step 2*** Establish a rectangular dielectric substrate with a certain thickness based on the operating wavelength, with a. recommended length and width of 0.5λ.
***Step 3*** Select a portion of the image as a metal ground, and convert the pixels of the segmented 2D image into metal pixel patches with a length of λ/50 and a width of λ/50. Finally, we overlay these 2D metal ground images onto the dielectric substrates.
***Step 4*** Another portion of the image is selected as the radiation part of the antenna, and converts the pixels of the segmented 2D image into metal pixel patches with a length of λ/25 mm and a width of λ/25 –0.08 mm. Subsequently, map the 2D metal radiation patch images onto the dielectric substrates.
***Step 5*** Determine the antenna feeding position.

## Optimization of antenna geometry

The antenna geometry is then searched through optimization to meet the design specifications. The conventional approach is to obtain the antenna response through full electromagnetic simulation, but for such a large search space, this approach faces challenges, because the full electromagnetic simulation is not quite computational efficient. A more computationally efficient surrogate model, known as the internal multi-port method, is used to simulate the characteristics of the antenna.

In the extracted and pixelated physical model, ports are assigned between adjacent pixels. Through full electromagnetic simulation of the pixel initial structure in Fig. 1 b, the impedance matrix of all ports of the pixel initial structure is obtained. This impedance matrix represents the multi-port network model, as illustrated in Fig. 1c, which serves as an efficient and high-precision approximation model of the full electromagnetic simulation model. The multi-port network model is employed for each evaluation of the objective function during the optimization process.

Figure 2 illustrates a schematic of the internal ports and the multi-port network. The ports are categorized into internal and external ports. External ports are utilized to feed the antenna structure, and the state of the internal ports determines the topology of the antenna. The states of the internal ports are either open ($Z_{Li}$=∞) or short ($Z_{Li}$=0). Short circuit is carried by small metal patches, and different combinations of short circuits on internal ports can change the current topology of the antenna, thereby optimizing its performance.

Figure 2 shows a structure with 1 external port and $N$ internal ports. The impedance metrix of the entire structure is defined by

$$\mathbf{Z}_a = \begin{bmatrix} \mathbf{Z}_{00} & \mathbf{Z}_{1N} \\ \mathbf{Z}_{N1} & \mathbf{Z}_{NN} \end{bmatrix} \tag{3}$$

,

where $\mathbf{Z}_{ij}(\omega)$, $i$, $j \in [0, N]$ are block matrixes. $\mathbf{Z}_{1N}$ and $\mathbf{Z}_{N1}$ represents the mutual impedance between loads ports and feeding port. $\mathbf{Z}_{00}$, and $\mathbf{Z}_{NN}$ represents self-impedance of the feeding port and internal ports, respectively.

The input impedance of the antenna is calculated by Eq. (4).

$$Z_s = \frac{v_0}{i_0} = \mathbf{Z}_{00} - \mathbf{Z}_{1N} \cdot (\mathbf{Z}_L + \mathbf{Z}_{NN})^{-1} \cdot \mathbf{Z}_{N1} \tag{4}$$

.

Then, we obtain the reflection coefficient of the antenna by

$$S_{11} = \frac{\mathbf{Z}_{00} - \mathbf{Z}_{1N} \cdot (\mathbf{Z}_L + \mathbf{Z}_{NN})^{-1} \cdot \mathbf{Z}_{N1} - Z_0}{\mathbf{Z}_{00} - \mathbf{Z}_{1N} \cdot (\mathbf{Z}_L + \mathbf{Z}_{NN})^{-1} \cdot \mathbf{Z}_{N1} + Z_0} \tag{5}$$

.

We can adjust the performance of the antenna based on the load of the internal port $\boldsymbol{Z}_L$ using Eq. (5). In order to optimize antenna performance, the loads on internal ports can be changed. So, we set the design variables $\boldsymbol{x}$

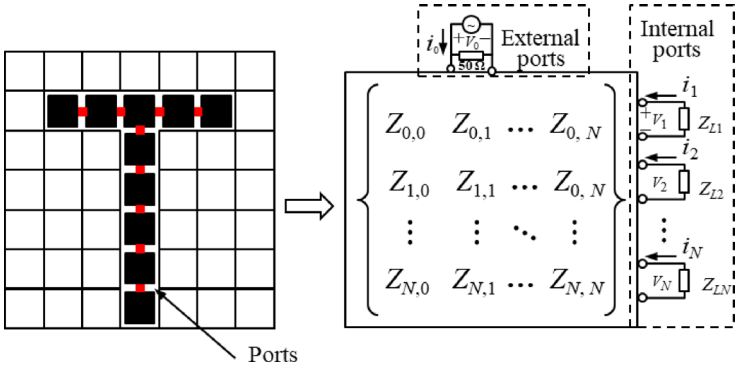


**Fig. 2**. Physical model using multiport networks of initial structure for patch antennas.

=[$Z_{L1}$, $Z_{L2}$,…, $Z_{LN}$], which is a vector representing the states of all internal ports, in which "0" represents "open" and "1" represents "short". The objective function for optimizing antenna performance is defined as

$$\mathbf{x}^* = \arg\min \sum_{k=1}^{K} \sum_{l=1}^{L} \left| |S_{11}(\mathbf{x}, f_{k,l})|_{\mathrm{dB}}, T_k \right|^* \quad s.\ t.\ x \in \{0,1\}^N \tag{6}$$

,

where $k$ is the index of the frequency band that we are interested in, and $l$ is the index of the frequency point within each frequency band. $T_k$ is the required threshold for band $k$, and $L_k$ is the number of sampling frequency points in band $k$. If $a > b$, $|a, b|^*=1$, otherwise $|a, b|^*=0$. $|S_{11}(\boldsymbol{x}, f_{k,l})|_{\mathrm{dB}}$ refers to the magnitude of the scalar $S$-parameter in dB. Here, the design variables only have two possibilities: 0 and 1, making it a typical binary optimization problem.

Genetic algorithm shows remarkable advantages in 0–1 code optimization problems, which can carry out global search in a large search space and effectively avoid falling into local optimal solutions. At the same time, the algorithm has strong robustness and is not easily affected by various factors. Therefore, genetic algorithm is particularly suitable for solving 0–1 code optimization problems, especially for classical NP-hard problems such as pixel antenna structure topology optimization. Standard GA is utilized in our work with a population size of 1000 across 200 generations. The probability of crossover is 0.8, and the probability of variation is 0.01. The detailed design structure, as well as the simulation and measured results, are presented comprehensively in Section III.

## Results

To evaluate the effectiveness of the proposed method, we first consider an example involving the design of a logo antenna that covers three frequency bands of WiFi 2.4 GHz (2.4–2.5 GHz), LTE FDD Band 3400 (3.4–3.5 GHz), and FR1 n79 band (4.7–4.9 GHz).

### Structure of the patch antenna

The components of the badge antenna for Guangzhou University is shown in Fig. 3. Figure 3 is depicted as an expanded-view illustration, where the feeding port, the ring-shaped ground, the radiation patch, and the substrate are arranged at distinct planar levels. In contrast, within the actual model, the feeding port, the ground, and the radiation patch are all located on the left-hand side of the substrate, with no metallic material present on the right-hand side. The substrate is defined as FR4, with a thickness of 1.6 mm, a relative dielectric constant of 4.33, and size of 60 mm×60 mm. The feeding port is positioned between the bottom pixel of the radiator and the closest point of the outer ring ground, as shown in Fig. 4. The metal ground consists of pixels measuring 0.24 mm×0.24 mm, and the metallic radiator comprises pixels measuring 0.48 mm × 0.40 mm. The outer ring of the logo retains its initial form, free from pixelation. Our experimental findings reveal that pixelating the outer ring poses several issues: Firstly, it compromises the aesthetic appeal of the overall design, as the complete structure of the outer ring appears more visually pleasing compared to a pixelated structure. Additionally, pixelating the outer ring results in a significant increase in the number of ports and consequently, a dramatic expansion of the search space, thereby increasing the complexity of design and optimization.

The inner metal patch is pixelated, resulting in about 1000 pixel elements. In order to reduce the search space, the internal port settings are as shown in Fig. 4. Figure 4a displays the configuration of the internal ports, whereas Fig. 4b presents the numbering of all 188 internal ports. The numbering starts from the left and moving right, then moving from the bottom to the top.

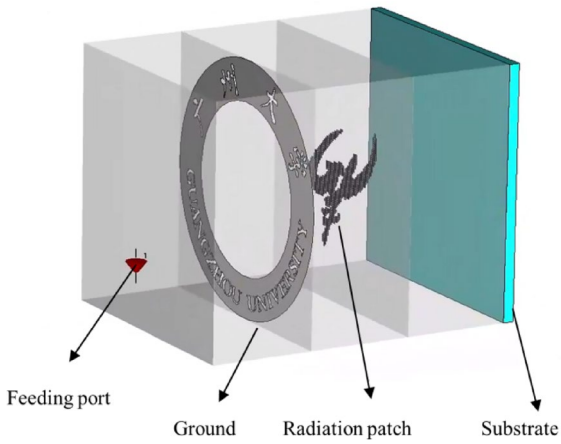


**Fig. 3**. Components of the badge antenna for Guangzhou University.

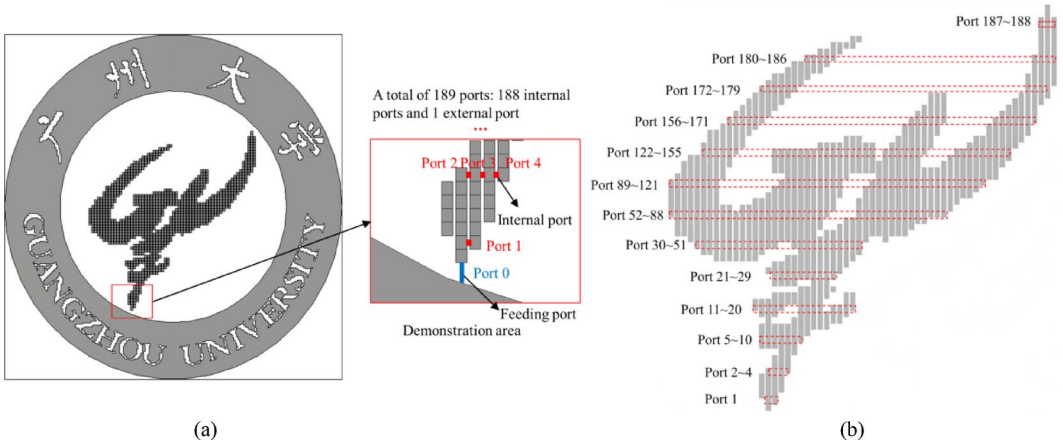


**Fig. 4**. Radiation patch with (**a**) internal port settings (**b**) port numbering of 188 internal ports.

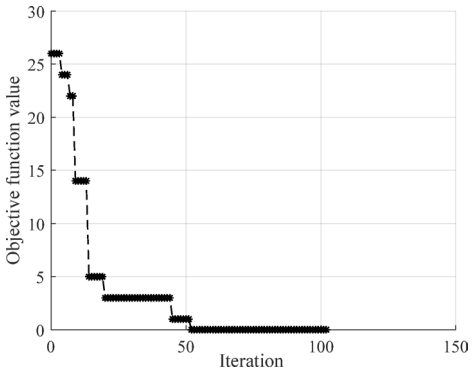


**Fig. 5**. Convergence curves of the optimization process for the tri-band patch antenna.

| | |
|---|---|
| Shorted ports | 1 2 3 5 6 7 8 9 13 16 20 22 23 24 25 27 29 32 33 34 35 37 38 39 40 41 43 45 46 47 49 55 56 57 58 59 61 62 63 65 68 69 72 73 74 76 78 79 80 82 83 84 85 86 88 89 91 95 96 101 103 104 107 109 110 113 115 117 118 123 124 125 127 129 130 134 137 138 140 144 147 152 153 154 155 156 158 161 166 167 169 172 173 175 178 181 183 184 188 |
| Open ports | 4 10 11 12 14 15 17 18 19 21 26 28 30 31 36 42 44 48 50 51 52 53 54 60 64 66 67 70 71 75 77 81 87 90 92 93 94 97 98 99 100 102 105 106 108 111 112 114 116 119 120 121 122 126 128 131 132 13 135 136 139 141 142 143 145 146 148 149 150 151 157 159 160 162 163 164 165 168 170 171 174 176 177 179 180 182 185 186 187 |

**Table 1**. States of all 188 ports of the tri-band patch antenna.

## Simulated and measured results

The design specification requires the return loss to be lower than -10dB across the three bands that covers 2.4–2.5 GHz, 3.30–3.40 GHz, and 4.7–5 GHz. Genetic algorithm (GA) is utilized to optimize the performance of the tri-band antenna, the evolution curve is as shown in Fig. 5. The optimal internal port state parameters obtained are presented in Table 1. When compared with Fig. 4(b), the states of each port and their corresponding geometric positions are clearly understandable.

The current distribution and far-field patterns of the antenna are simulated, as shown in Figs. 6 and 7. It can be observed that the current distribution and far-field patterns of the antenna are influenced by both frequency and antenna structure. By optimizing the antenna structure and adjusting the current distribution, improved radiation characteristics can be achieved. The entire optimization process, including multi-port parameter extraction, multi-port network modeling and antenna performance optimization, took about two hours. If try to optimize the electromagnetic simulation model directly using conventional algorithms, it is almost impossible to find a solution that meets the design requirements. The results show that the proposed method is effective for antenna design.

A prototype of the tri-band patch antenna has been fabricated. The detailed structural geometry, with the shorted ports marked, and the prototype itself are presented in Fig. 8a and b, respectively. The $S_{11}$ parameters of the antenna are illustrated in Fig. 9. It is noted that the performance of the optimized antenna is excellent, as verified through simulations and measurements, indicating that the antenna exhibits good performance. The measured results are highly consistent with the EM simulation and multi-port model results, and meet the – 10

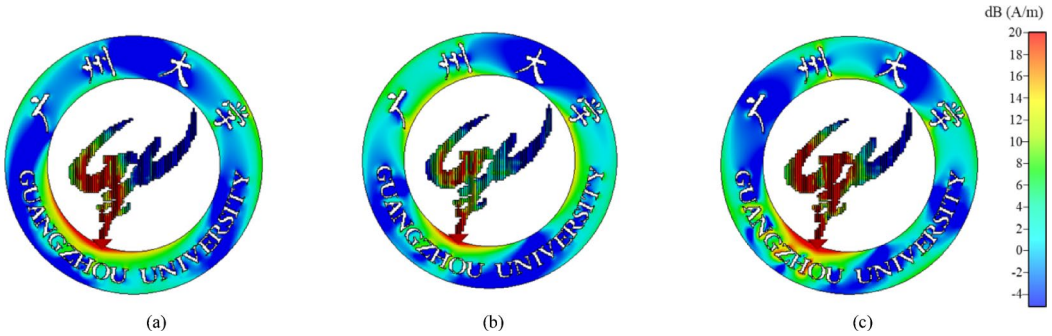


**Fig. 6**. Current distribution of the antenna (**a**), 2.45 GHz, (**b**) 3.35 GHz and (**c**) 4.85 GHz.

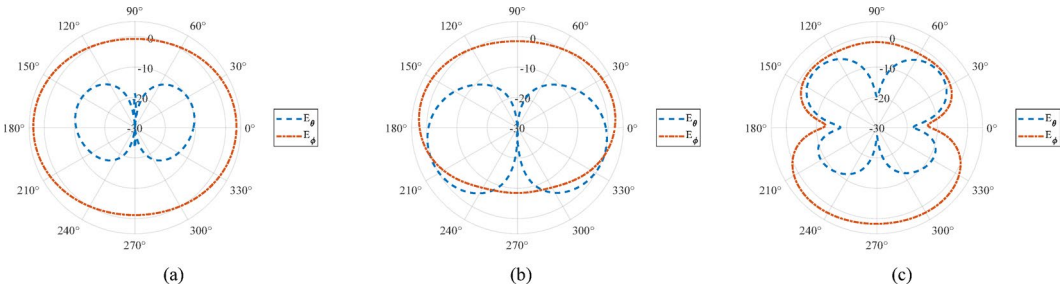


**Fig. 7**. Simulated far-field pattern of the antenna (**a**) 2.45 GHz, (**b**) 3.35 GHz and (**c**) 4.85 GHz.

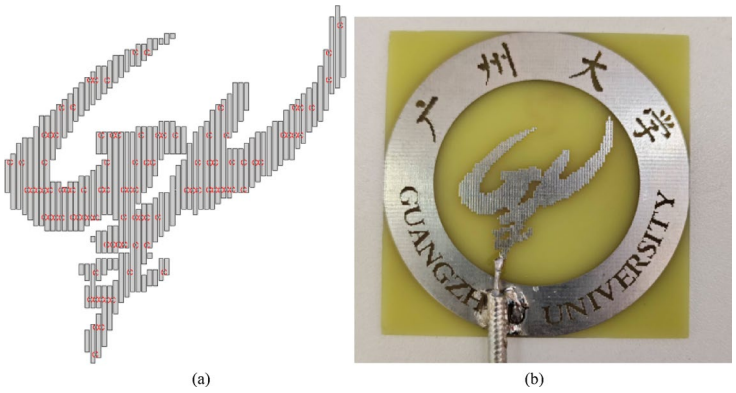


**Fig. 8**. (**a**) Detailed structure geometry with shorted ports marked and (**b**) Prototype of the tri-band patch antenna.

dB requirement in all frequency bands of interest. The simulated – 10 dB bandwidths of the three target frequency bands reached 310 MHz (2.24 GHz to 2.55 GHz), 860 MHz (3.3 GHz to 4.24 GHz), and 340 MHz (4.66 GHz to 5 GHz) respectively, while the measured bandwidths are 140 MHz (2.37 GHz to 2.51 GHz), 1100 MHz (3.3 GHz to 4.4 GHz), and 360 MHz (4.64 GHz to 5 GHz).

Figure 9(b) shows realized gain and efficiency curves, revealing a strong agreement between efficiency/gain and the S-parameter plots. The frequency band with high efficiency and gain closely overlap those exhibiting optimal impedance matching (from S-parameters). Across the target frequency bands, efficiency exceeds 75%, with distinct performance highlights: in the first band, gain surpasses 3.65 dB at >90% efficiency; in the second band, both gain (>4.6 dB) and efficiency (>90%) peak further; and in the third band, efficiency remains above 75% while gain exceeds 3 dB.

## Comparison

Table 2 compares this work with related studies, evaluating antenna type, feeding ports, operating bands, polarization, relative bandwidth, gain, and efficiency. Notably[5], employs a sleeve badge-derived circularly polarized antenna with 5.6% bandwidth and 5.04 dBi gain but low efficiency (55.3%);[6] introduces a military-use textile antenna with 26% bandwidth, 5.2 dBi gain, and 79.2% efficiency;[7] presents a dual-band textile antenna

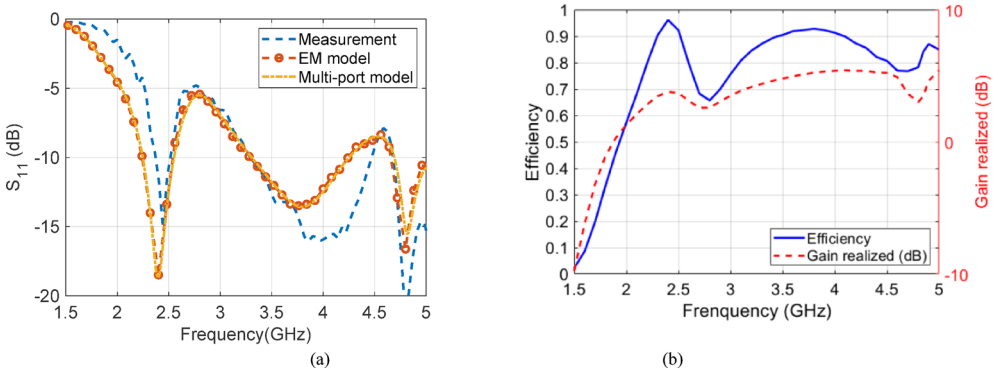


**Fig. 9**. (**a**) Optimized *S*-parameter (**b**) efficiency and gain curves of the tri-band antenna.

| References | Ant. type | No. of port | No. of band | Polarization | FBW (%) | Gain (dBi) | Efficiency |
|---|---|---|---|---|---|---|---|
| [5] | Sleeve-Badge | 1 | 1 | CP | 5.6% | 5.04 | 55.3% |
| [6] | All textile for military | 1 | 1 | LP | 26% | 5.2 | 79.2% |
| [7] | All textile | 1 | 2 | LP | 17.1%/13% | -0.29/3.05 | NA |
| [15] | mm-wave patch | 16 | 1 | LP | 11.45% | 19.2 | NA |
| This work | Pixel and patch | 1 | 3 | LP | 12.9%/ 22.8%/7.0% | 3.6/4.6/3.0 | 75% |

**Table 2**. Comparison with other related works.

inspired by the LV logo, achieving 17.1%/13% bandwidths and −0.29/3.05 dBi gains; and[15] features a 16-unit millimeter-wave patch antenna array shaped as Chinese characters, with 11.45% bandwidth and 19.2 dBi gain. In contrast, this work pixelates a university emblem into a tri-band antenna via optimized pixel connectivity, offering 12.9%/22.8%/7.0% bandwidths, 3.6/4.6/3.0 dBi gains, and > 75% efficiency using a patch antenna design. Next, new manufacturing processes such as textile materials or other soft wearable materials will be attempted to further promote its application in the field of the Internet of Things.

## Conclusions

The advancement of IoT drives the demand for increasingly compact electronic devices, and in this work we introduced an innovative solution: the design of a predefined shape that serves dual functionality as an antenna while preserving its original aesthetic form. In this proposed method, the image segmentation technique is used to extract the predefined shape for the patch antenna. Some of the metallic parts are pixelated, and then the connection states between adjacent pixels are designed through optimization to meet the design specification. A cost-efficient multi-port network model is employed to significantly reduce the computational cost associated with EM simulations during the optimization of antenna performance. To verify the effectiveness of our proposed method, we design an antenna operating across the bands of WiFi 2.4 GHz (2.4–2.5 GHz), LTE FDD Band 3400 (3.4–3.5 GHz), and FR1 n79 band (4.7–4.9 GHz), based on the badge of Guangzhou University. The resulting patch antenna, which maintains the visual resemblance to the university emblem, attains bandwidths of 12.9%, 22.8%, and 7.0%, along with gains of 3.6 dBi, 4.6 dBi, and 3.0 dBi, and an efficiency exceeding 75%. These results serve to validate the effectiveness of the proposed method.

## Data availability

The datasets used and/or analysed during the current study available from the corresponding author on reasonable request.

Received: 5 August 2024; Accepted: 11 June 2025
Published online: 02 July 2025

## References

1. Abbasi, N. A. et al. High-Isolation array antenna design for 5G mm-Wave MIMO applications. *J. Infrared Milli Terahz Waves*. **46**, 12. https://doi.org/10.1007/s10762-024-01027-3 (2025).
2. Althuwayb, A. A. et al. Metasurface-inspired flexible wearable MIMO antenna array for wireless body area network applications and biomedical telemetry devices. *IEEE Access*. **11**, 1039–1056. https://doi.org/10.1109/ACCESS.2022.3233388 (2022).
3. Althuwayb, A. A. et al. Design technique to mitigate unwanted coupling in densely packed radiating elements of an antenna array for electronic devices and wireless communication systems operating in the millimeter-wave band. *AEU-International J. Electron. Commun.* **159**, 154464. https://doi.org/10.1016/j.aeue.2022.154464 (2023).
4. Alibakhshikenari, M. et al. Virtual antenna array for reduced energy per bit transmission at Sub-5 ghz mobile wireless communication systems. *Alexandria Eng. J.* **71**, 439–450. https://doi.org/10.1016/j.aej.2023.03.056 (2023).

5. Joler, B. M. Maja.A. sleeve-badge circularly polarized textile antenna. *IEEE Trans. Antennas and Propagation*, 66(99):1576–1579. (2018). https://doi.org/10.1109/TAP.2018.2794420(2018).
6. Çelenk, E. & Tokan, N. T. All-textile on-body antenna for military applications. *IEEE Antennas. Wirel. Propag. Lett.* **21** (5), 1065–1069. https://doi.org/10.1109/LAWP.2022.3159301 (2022).
7. Tak, J. & Choi, J. A. All-Textile Louis Vuitton logo antenna. *IEEE Antennas. Wirel. Propag. Lett.* **14**, 1211–1214. https://doi.org/10.1109/LAWP.2015.2398854 (2015).
8. Li, J. et al. A multi-band automotive LOGO antenna. *IEEE 11th Asia-Pacific Conference on Antennas and Propagation (APCAP)*, Guangzhou, China, 2023:1–2, Guangzhou, China, 2023:1–2, (2023). https://doi.org/10.1109/APCAP59480.2023.10470237(2023).
9. Fang, X. S. & Leung, K. W. Aesthetic transparent dielectric resonator antenna with omnidirectional radiation pattern. *Proceedings of the 2012 IEEE International Symposium on Antennas and Propagation*, Chicago, IL, USA, 2012:1–2, (2012). https://doi.org/10.1109/APS.2012.6348955
10. Atanasov, B., Atanasov, N. & Atanasova, G. A multi-band antenna with an aesthetic design for ambient rf energy harvesting. *17th European Conference on Antennas and Propagation (EuCAP)*, Florence, Italy, 2023:1–5, Florence, Italy, 2023:1–5, (2023). https://doi.org/10.23919/EuCAP57121.2023.10133321(2023).
11. Nie, L. Y. et al. Wideband design of a compact monopole-like circular patch antenna using modal analysis. *IEEE Antennas. Wirel. Propag. Lett.* **20** (6), 918–922. https://doi.org/10.1109/LAWP.2021.3066985 (2021).
12. Sun, C. A design of compact ultrawideband circularly polarized microstrip patch antenna. *IEEE Trans. Antennas Propag.* **67** (9), 6170–6175. https://doi.org/10.1109/TAP.2019.2922759 (2019).
13. Chen, C. A single-layer single-patch dual-polarized high-gain cross-shaped microstrip patch antenna. *IEEE Antennas. Wirel. Propag. Lett.* **22** (10), 2417–2421. https://doi.org/10.1109/LAWP.2023.3289861 (2023).
14. Mitha, T. & Pour M.Investigation of dominant transverse electric mode in microstrip patch antennas. *IEEE Trans. Antennas Propag.* **67** (1), 643–648. https://doi.org/10.1109/tap.2018.2874765 (2019).
15. Feng, B., Chen, J. & Sim, C. Y. D. Analysis of double-Xi-shaped millimetre-wave patch antenna backed by a high-order-mode cavity using characteristic mode design. *IET Microwaves Antennas Propag.* **2021** (8), 15. https://doi.org/10.1049/mia2.12118 (2021).
16. Chung, K. L. et al. A circular-polarization reconfigurable meng-shaped patch antenna. *IEEE Access.* **2018** (6). https://doi.org/10.1109/ACCESS.2018.2869410 (2018).
17. Koziel, S. & Pietrenko-Dabrowska, A. Efficient simulation-based global antenna optimization using characteristic point method and nature-inspired metaheuristics. *IEEE Trans. Antennas Propag.* **72** (4), 3706–3717. https://doi.org/10.1109/TAP.2024.3370296J( (2024).
18. O'Brien, M., Grandfield, J. E., Mumcu, G. & Weller, T. M. Miniaturization of a spiral antenna using periodic z-plane meandering. *IEEE Trans. Antennas Propag.* **63** (4), 1843–1848. https://doi.org/10.1109/TAP.2015.2394796 (2015).
19. Van Aarle, W. & Batenburg, K. J. Sijbers J.Optimal threshold selection for segmentation of dense homogeneous objects in tomographic reconstructions. *IEEE Transactions on Medical Imaging*, 30(4):980. (2011). https://doi.org/10.1109/TMI.2010.2104328(2010).
20. Abdulrahman, A. & Varol, S. A Review of image segmentation using matlab environment. (2020). https://doi.org/10.1109/ISDFS49300.2020.9116191 (2020).
21. Jiang, F. et al. Pixel antenna optimization using n-port characteristic mode analysis. *IEEE Trans. Antennas Propag.* **68** (5), 3336–3347. https://doi.org/10.1109/TAP.2019.2963588 (2020).
22. Jiang, F. et al. Multiport pixel antenna optimization using characteristic mode analysis and sequential feeding Port search. *IEEE Trans. Antennas Propag.* **70** (10), 9160–9174. https://doi.org/10.1109/TAP.2022.3184489 (2022).
23. Jing, L., Li, M. & Murch, R. Compact pattern reconfigurable pixel antenna with diagonal pixel connections. *IEEE Trans. Antennas Propag.* **70** (10), 8951–8961. https://doi.org/10.1109/TAP.2022.3177499 (2022).


## Acknowledgements

This work was supported in part by the State Key Laboratory of Millimeter Waves, Southeast University (K202403) and in part by Special Topic on Basic and Applied Basic Research in Guangzhou, Young Doctoral "Sailing" Project, (2024A04J3520)

## Author contributions

Fan Jiang is responsible for multi-objective algorithm design and antenna design. Zhen Zhang is responsible for the framework of this work. Bo Liu and Weihua Yu are responsible for checking the grammar of this work.

## Declarations

## Competing interests

The authors declare no competing interests.

## Additional information

**Supplementary Information** The online version contains supplementary material available at https://doi.org/10.1038/s41598-025-06781-5.

**Correspondence** and requests for materials should be addressed to Z.Z. or W.Y.